

IN SITU PHOTOCHEMICAL CROSSLINKING OF HYDROGEL MEMBRANE FOR GUIDED TISSUE REGENERATION

Pauline Marie Chichiricco ^{a,b}, Raphaël Riva^a, Jean-Michel Thomassin^a, Julie Lesoeur^{b,c,d}, Xavier Struillou^{b,c,e}, Catherine Le Visage^{b,c}, Christine Jérôme^{a,1}, Pierre Weiss^{b,c,e,*}, ¹

^a Center for Education and Research on Macromolecules (CERM), CESAM Research Unit, University of Liège, B-4000 Liège, Belgium

^b Inserm, UMR 1229, RMeS, Regenerative Medicine and Skeleton, Université de Nantes, ONIRIS, Nantes, F-44042, France

^c Université de Nantes, UFR Odontologie, Nantes, F-44042, France

^d INSERM, UMS 016, CNRS 3556, Structure Fédérative de Recherche François Bonamy, SC3M facility, CHU Nantes, Université de Nantes, Nantes, F-44042, France

^e CHU Nantes, PHU4 OTONN, Nantes, F-44093, France

*Corresponding author at: RMES Lab, 1 place A. Ricordeau, 44042 Nantes, cedex 01.

E-mail address: pierre.weiss@univ-nantes.fr (P. Weiss).

¹ Christine Jérôme and Pierre Weiss are co-last authors.

KEYWORDS: PHOTOCROSSLINKING -- DENTAL BIOMATERIAL -- PERIODONTITIS -- CHITOSAN -- RIBOFLAVIN -- CARBOXYMETHYL CHITOSAN -- SILANIZED HYDROXYPROPYL METHYLCELLULOSE -- INTERPENETRATED POLYMER NETWORK -- BARRIER MEMBRANE -- VISIBLE LIGHT PHOTOPOLYMERIZATION

ABSTRACT

Objective. Periodontitis is an inflammatory disease that destroys the tooth-supporting attachment apparatus. Guided tissue regeneration (GTR) is a technique based on a barrier membrane designed to prevent wound space colonization by gingival cells. This study examined a new formulation composed of two polymers that could be photochemically cross-linked *in situ* into an interpenetrated polymer network (IPN) forming a hydrogel membrane.

Methods. We synthesized and characterized silanized hydroxypropyl methylcellulose (Si-HPMC) for its cell barrier properties and methacrylated carboxymethyl chitosan (MA-CMCS) for its degradable backbone to use in IPN. Hydrogel membranes were cross-linked using riboflavin photoinitiator and a dentistry visible light lamp. The biomaterial's physicochemical and mechanical properties were determined. Hydrogel membrane degradation was evaluated in lysozyme. Cytocompatibility was estimated by neutral red uptake. The cell barrier property was studied culturing human primary gingival fibroblasts or human gingival explants on membrane and analyzed with confocal microscopy and histological staining.

Results. The IPN hydrogel membrane was obtained after 120 s of irradiation. The IPN showed a synergistic increase in Young moduli compared with the single networks. The CMCS addition in IPN allows a progressive weight loss compared to each polymer network. Cytocompatibility was confirmed by neutral red assay. Human cell invasion was prevented by hydrogel membranes and

histological sections revealed that the biomaterial exhibited a barrier effect in contact with soft gingival tissue.

Significance. We demonstrated the ability of an innovative polymer formulation to form *in situ*, using a dentist's lamp, an IPN hydrogel membrane, which could be an easy-to-use biomaterial for GTR therapy.

1. Introduction

Oral diseases, including dental caries and periodontitis, are among the most important global health burdens, affecting the majority of school-aged children and adults worldwide. The prevalence of periodontitis is reported to be between 20 and 50% of the worldwide population [1], with reported relationships between periodontitis and systemic diseases such as cardiovascular disease [2], [3]. In Europe, the more severe forms of periodontitis affect 10% of the population [4].

Periodontitis is an inflammatory disease resulting from the presence of oral bacteria biofilm in the periodontal tissue, which leads to an immune-inflammatory response and destroys the tooth-supporting attachment apparatus [5]. The inflammation, if untreated, can spread to the whole gum and all periodontal tissues leading to the destruction of periodontal ligament and loss of the supporting tooth bone with ultimately the risk of spontaneous avulsion of the tooth [6]. For more severe cases, the dentist or periodontist generally selects a surgical approach that allows the elimination of periodontal pockets and the partial regeneration of the lost tissues with the use of various biomaterials. Several regenerative procedures have already been introduced to clinical practice to overcome these problems, including bone grafts, guided tissue regeneration (GTR), enamel matrix derivative and combined techniques [7].

GTR is a dental surgical procedure to regenerate lost components of periodontium. In this technique a biocompatible membrane is implanted around the periodontal lesion in order to prevent its colonization by soft tissues presenting a faster proliferation rate compared to the bone and ligament cells. In fact, during normal healing, it appears that the soft tissue migrates rapidly into the wound, avoiding tissue regeneration. The barrier membrane plays a key role in preventing undesirable tissue migration into the defective area, and consequently, it allows sufficient time for bone, cementum, and periodontal ligament regeneration.

For this purpose, the membrane, whether or not it is resorbable, must be biocompatible to prevent inflammatory processes and must present a selective permeability allowing the diffusion of nutrients without the passage of cells with an appropriated flexibility, compatible with the anatomical implantation. Among the nonresorbable membranes, polytetrafluoroethylene (e.g., Cytoplast[®] TXT-200, Osteogenics Biomedical) –based membranes are widely used, although a second surgery for their removal after use is mandatory. These nonresorbable membranes present high postoperative morbidity. To overcome this limitation, resorbable membranes, made from biodegradable materials, are largely studied to obviate the need for a second surgery and thus reduce complications (e.g., Bio-Gide[®], Osteohealth) [7]. Nevertheless, the main drawback of resorbable membranes is their poor predictability in terms of resorption time largely influenced by the patient's characteristics. Generally, these membranes are made of polylactic acid, polyglycolic, polyurethane, collagen type I, etc. [8], [9]. Most resorbable membranes used to date are characterized by rapid absorption kinetics after implantation. In fact, these membranes do not ensure, for a period of 8 weeks or more, the regenerating process below the barrier. To improve their properties, commercially available membranes are generally made of a cross-linked polymer given that the presence of physical or chemical crosslinking nodes delays the loss of barrier properties [8].

In addition, it should be taken into account that all the membranes now available are in a solid form, requiring skill and experience to be perfectly applied in narrow defects [10].

For complicated shapes or for a defect that is difficult to reach, liquid formulations, able to form solid membrane *in situ*, are easy-to-use materials that save time and money. To our knowledge, two kinds of free-flow membranes have been commercialized: Membragel® (Straumann, Austria) and Atrisorb® (Tolmar, USA), but they are no longer available according to the manufacturers [7]. The first one is composed of multiarm PEG with thiol end-groups and acrylate end-groups that react forming a hydrogel membrane [11]. The second one is composed of poly(DL-lactide) (PLA) dissolved in *N*-methyl-2-pyrrolidone (NMP) [12].

Si-HPMC is a self-setting hydrogel that has been reported in the literature for many biological applications. It has the advantage of being injected as a viscous solution and then, due to the condensation reaction, it builds a 3D network *in situ*. This material was demonstrated to be biocompatible and slowly degraded in a rabbit model [13], [14], [15], [16]. In addition, Struillou et al. demonstrated the capability of the cross-linked biomaterial to act as a physical barrier against cell invasion [17]. The main drawback of this self-setting hydrogel is an excessively slow crosslinking process for clinical needs.

We have developed an original mixture of biomaterials that could be used as a liquid formulation, a precursor of a resorbable interpenetrated polymer network hydrogel membrane formed by *in situ* curing under irradiation with a dentist's lamp. Indeed, photo-curing appears to be the most appropriate technique for this application given both its shape and the control of the curing time, and it has been reported in the literature for tissue engineering, cell encapsulation and drug delivery [18], [19], [20], [21].

For several decades, interpenetrating polymer networks have been widely used because of the synergistic combination of each of the polymer networks [20], [22], [23]. Our membrane is composed of a Si-HPMC network, selected for its appropriate barrier effect against soft tissue invasion, which is interpenetrated in a methacrylated carboxymethyl chitosan network (MA-CMCS). Carboxymethyl chitosan allows the modification of membrane degradation due to its degradable backbone. This biocompatible and biodegradable polysaccharide, derived from natural chitin, is water soluble at neutral pH and presents antibacterial properties [24], [25]. To allow photocrosslinking, methacrylate functions were randomly introduced along the CMCS backbone to provide the gelation under visible light irradiation using a photoinitiator solution (PIS) based on vitamin B2 [26], [27], [28]. Vitamin B2, or riboflavin, is a water-soluble vitamin widely present in both animal- and plant-derived foods [20]. In particular, we used its highly water-soluble riboflavin 5'-phosphate sodium salt hydrate derivative (RP); since it is a type II photoinitiator, it requires the addition of triethanolamine as a coinitiator.

The aim of this study was to associate the Si-HPMC and MA-CMCS polymers in an injectable viscous solution able to quickly gel under light irradiation into a biocompatible and resorbable hydrogel membrane for GTR.

This new formulation was analyzed from a chemical and rheological point of view. The cell viability and barrier membrane effect were evaluated with soft tissue cells and *ex vivo* gingiva cultures.

Table 1. Macromolecular parameters of the polysaccharide precursors.

Carboxymethyl chitosan (HMC + Heppe Medical Chitosan GmbH)	Degree of deacetylation 94.2% Viscosity (1% water 20 °C) 22 mPas Molecular weight (from GPC) 30–500 kDa
Hydroxypropyl methylcellulose Methocel E4M (Colorcon)	Viscosity (2% water 20 °C) 3.023 mPas Methoxyl groups 28.2% Hydroxypropyl groups 9.3%

2. Materials and methods

2.1. MATERIALS

Carboxymethyl chitosan (CMCS) was purchased from Heppe Medical Chitosan GmbH (Halle, Germany). Riboflavin 5phosphate sodium salt hydrate (RP), triethanolamine (TEOHA), glycidyl methacrylate, dimethylsulfoxide (DMSO), HEPES (4-(2-hydroxyethyl) piperazine-1-ethanesulfonic acid), lysozyme (from chicken egg whites), RNase, paraformaldehyde and neutral red were all obtained from Sigma Aldrich (Saint Louis, MO, USA). Hydroxypropyl methylcellulose (HPMC) was provided by Colorcon-Dow Chemical (Harleysville, PA, USA). Fetal bovine serum (FBS) was acquired from PAN biotech GmbH (Aidenbach, Germany). Penicillin, streptomycin, trypsin-EDTA, DMEM and phosphate buffered saline (PBS) were obtained from Gibco (Invitrogen, Carlsbad, CA, USA) and L929 cells from ATCC (Manassas, VA, USA). YOYO -1 iodide (491/509) and Alexa Fluor 568 phalloidin were purchased from Thermo Fisher (Waltham, MA, USA). Harris Hematoxylin and Eosin Y were obtained from Surgipath (Richmond, IL, USA) and Safranin from VWR (Radnor, PA, USA) The macromolecule parameters of CMCS and HPMC are listed in the Table 1.

2.2. METHODS

2.2.1. Si-HPMC SYNTHESIS

Si-HPMC was synthesized by grafting 3glycidoxypropyltrimethoxysilane to HPMC as described elsewhere [30,31]. Then Si-HPMC powder was dissolved in 0.1 M NaOH overnight and sterilized by autoclave (121° C for 20 min) as previously described [32].

2.2.2. MA-CMCS SYNTHESIS

Ten grams of CMCS was dissolved in 500 mL of Milli-Q water under magnetic stirring and the pH was adjusted to 9 with a 0.1 M NaOH solution. A total of 2.72 mL of glycidyl methacrylate was then added to target a 40 mol% percentage of methacrylation. After 48 h of stirring at room temperature under nitrogen atmosphere, the reaction mixture was dialyzed against distilled water (porosity of

the dialysis membrane MWCO, 1 kDA, Spectrapor) until the conductivity was less than 2 S/cm before being freeze-dried for 3 days.

2.2.3. FT-IR

Infrared spectroscopy spectra were recorded with a Thermo Fisher Scientific Nicolet IS5 with module ATR ID5 in Germanium (700cm⁻¹–4000cm⁻¹). CMCS and MA-CMCS were analyzed in their lyophilized form.

2.2.4. ¹H NMR

The substitution degree was determined by ¹H NMR 400MHz at 80 °C (Bruker). The polysaccharide samples were solubilized in deuterium oxide at a concentration of 14 mg/mL. To calculate the grafting percentage, formula 1 was used:

$$\%MA = \frac{(DA/100) \times \int CH_3MA}{\int CH_3DA} \times 100 \quad (1)$$

where DA is the degree of residual acetylation on the chitosan backbone, CH_{3MA} is the integral of the methyl group of the methacrylate moiety ($\delta = 2.5$ ppm) and CH_{3DA} is the integral of the methyl group of the acetyl group in carboxymethyl chitosan ($\delta = 2.6$ ppm).

2.2.5. LIQUID FORMULATION PREPARATION

IPN precursor solution was prepared in a four-step procedure:

(1) Si-HPMC solution preparation, (2) acid buffer preparation, (3) MA-CMCS solution preparation and (4) a mixing step to obtain the Si-HPMC/MA-CMCS solution. The main steps are described as follows:

- (1) Si-HPMC was dissolved in 0.1 M NaOH at 4% (w/v).
- (2) Acid buffer was prepared with 0.06 M HCl, 1.8% (w/v) NaCl and 6.2% (w/v) HEPES.
- (3) MA-CMCS was dissolved in distilled water at 5% (w/v). To allow the crosslinking under irradiation, 5 L of PIS was added to the MA-CMCS per each final milliliter of total solution (stock solution of photoinitiator composed of RP 4.2 mM and 4.2 M of TEOHA [27]).
- (4) MA-CMCS, Si-HPMC and acid buffer were successively mixed in a 4:2:1 ratio in volume to obtain a 4% (w/v) solution.

To allow the correct comparison within different samples, Si-HPMC and MA-CMCS solutions were prepared at the same final concentration present in Si-HPMC/MA-CMCS formulation (1.14% (w/v) and 2.86% (w/v)).

2.2.6. HYDROGEL PREPARATION

The Si-HPMC/MA-CMCS and MA-CMCS solutions were poured into a Teflon mold and irradiated for 120 s from one side by means of a BA-Optima 10 dentistry lamp curing light 1200mw/cm², 420–480nm (B.A. International, Northampton, UK). Si-HPMC was mixed with acid buffer, previously

described, and transferred to a mold. We used a Teflon mold measuring 25 mm in diameter and 4 mm high for rheological/mechanical analysis and 5 mm in diameter and 2 mm high for the *in vitro* test. The ratio chosen between the two polymers to compose the interpenetrating polymer network was previously assessed testing different ratios of polymer and photoinitiator. The formulation selected was the only one that provided the correct crosslink of MA-CMCS in a short time, even in presence of Si-HPMC. Si-HPMC is a self-setting hydrogel, which, due to the condensation reaction, builds a 3D network. Struillou et al. demonstrated the capability of this biomaterial to act as a physical barrier against cell invasion when it is fully cross-linked [17]. The main drawback of this self-setting hydrogel, for this application, is an overly slow crosslinking time. For the *in vitro* study, so that Si-HPMC could be compared with the other hydrogels, we used Si-HPMC cross-linked for 4 days in a mold. To maintain the same conditions for all samples, MA-CMCS and Si-HPMC/MA-CMCS were prepared as described previously and preserved 4 days before the *in vitro* tests.

2.2.7. RHEOLOGY

Rheological measurements were taken on an ARES G2 rheometer (TA Instruments). The data were collected using the TRIOS software. Time-sweep experiments were conducted (1% strain, 6.28 rad/s) using a parallel plate geometry (20 mm in diameter) with an upper transparent quartz plate, allowing the material to be irradiated with a lamp to follow the gelation (= 450 nm, 430 mW, 350 mA, royal blue).

2.2.8. COMPRESSION TEST

The hydrogel stiffness was obtained from uniaxial static compression. Mechanical compression was performed using Texture Analyzer (TA HD plus) with a 25 mm cylindrical aluminum probe run at 0.1 mm/s. The stress-strain curves were recorded and the compression modulus was derived as the slope divided by the corresponding cross-section of the hydrogel sample.

2.2.9. ENZYME DEGRADATION

Hydrogel membrane degradation was investigated by incubating the hydrogels in 5 mL of PBS buffer containing lysozyme from chicken white eggs (10 mg/mL) at 37 °C. The solvent was replaced twice a week. The samples were weighed at different time points, eliminating excess solvent. The weight loss, reported as a ratio of final over initial weight percent (W/W_0)%, was followed over a period of 24 days. Hydrogels pictures were taken at every time point. All the experiments were conducted in triplicate.

2.2.10. *IN VITRO* CELL VIABILITY

To evaluate cytocompatibility, a neutral red uptake assay was carried out with the exposure of murine fibroblasts (L929, ATCC, VA, USA) to (1) PIS, (2) MA-CMCS extract and (3) Si-HPMC, Si-HPMC/MA-CMCS and MA-CMCS hydrogel.

The cells were cultured in Dulbecco's modified Eagle's medium (DMEM) with 4.5 mg/mL glucose, 10% fetal bovine serum and 1% penicillin–streptomycin. Cells were detached by 0.2% trypsin and seeded 16,000 cells/mm² in a 96-well Plate 24 h before every test.

To perform the neutral red uptake assay, a solution was prepared 24 h before the test with 0.04 mg/mL of neutral red in PBS and incubated at 37 °C. Before being added to cells, the solution was centrifuged to remove any crystals. One hundred microliters of neutral red solution was added to cells and incubated for 3 h. After incubation, the solution was removed and a destain solution (50% ethanol 96%, 49% deionized water, 1% glacial acetic acid) was used to solubilize the dye trapped in living cells. The optical density was read at 550 nm using a microplate reader (Victor3 V, PerkinElmer, Wellesley, MA, USA). The averages of optical density units were calculated after blank subtraction.

All the tests were performed in triplicate. The results in neutral red uptake were expressed as the percentage of the ratio between the optical density of the experimental condition and the optical density of the control well, named untreated cells.

2.2.10.1. Photoinitiator solution. A PIS of 4.2 mM RP and 4.2 M of TEOHA [27] was prepared and HCl was added to neutralize the pH solution as in polymer liquid formulation [33]. In fact, although we analyzed only the impact of triethanolamine, as expected the unbalanced pH strongly impacted cell viability (data not shown). The PIS was added to culture medium at the same concentration as required for the polymer photocrosslinking (5 L/mL). To examine the effect of irradiation, visible light curing was used to expose cells containing or not containing the PIS for 120 s. Any plates not exposed at a given time were carefully covered to prevent any unregulated light exposure. After cell exposure to visible light, all the plates were returned to the 37 °C incubator for 24 h. The control well consisted of cells without PIS and not irradiated. After 24 h, the medium was removed, the cells rinsed with sterile PBS and neutral red solution added to each well plate to perform the assay.

2.2.10.2. MA-CMCS extract. MA-CMCS at 2% (w/v) was inserted in the dialysis tube (porosity of the dialysis membrane MWCO = 1 kDa, Spectrapor). The tube was introduced in a Falcon tube with 10 mL of distilled water under stirring at room temperature for 72 h. The extract, containing the polymer leach-out product, was sterilized on a 0.22- μ m filter and used for testing the effect of leach-out products on cell viability. The 96-well plates, incubated 24 h before with L929 cells, were recovered from the incubator. The culture medium was discarded and replaced with medium containing 10% (v/v) polymer extract. The control well consisted in cells with culture medium without polymer extract. To examine the effect of irradiation, visible light curing was used to expose cells containing or not containing polymer extract. After 1 and 3 days of incubation, the medium was removed, the cells rinsed with sterile PBS and neutral red solution added to each well plate to perform the assay.

2.2.10.3. Si-HPMC, MA-CMCS, Si-HPMC/MA-CMCS. Si-HPMC, Si-HPMC/MA-CMCS and MA-CMCS hydrogels were prepared as described in the Section 2.2.6. The 96-well plates, incubated 24 h before with L929 cells, were recovered from the incubator. The cell medium was removed and hydrogels were transferred in each well and successively covered with 100 μ L culture medium. The control well consisted in cells with 100 μ L culture medium without hydrogel. After 1 and 3 days, the hydrogels and the culture medium were removed, the cells rinsed with sterile PBS and neutral red solution added to each well plate to perform the assay.

2.2.11. *IN VITRO* BARRIER EFFECT

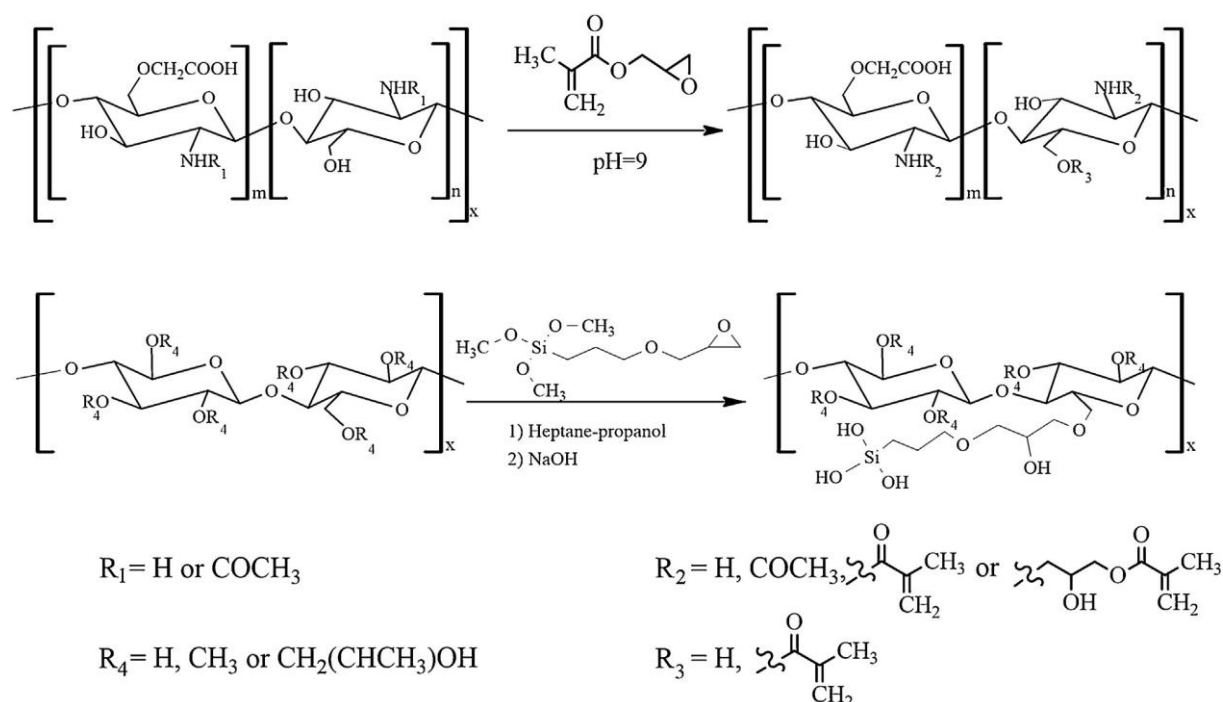
2.2.12. *EX VIVO* MODEL

Human gingival explant was obtained from a healthy patient undergoing dental surgery. The explant was rinsed three times in PBS with penicillin–streptomycin (2%) and divided into four samples. The explants were placed at the top of a porous pullulan/dextran hydrogel, Si-HMPC hydrogel, MA-CMCS hydrogel and Si-HMPC/MA-CMCS hydrogel membrane using a Teflon cylinder to maintain the contact for 1 week in 12-well plates and incubated with DMEM with 4.5 mg/mL glucose, 20% fetal bovine serum, 1% penicillin–streptomycin and 1% Fungizone. After culture, the explant/hydrogel samples were fixed with 4% PFA for 1 h, embedded in 30% sucrose solution and in OCT (optimal cutting temperature compound). Every sample was then frozen in isopentane with liquid nitrogen. After cryosectioning, the frozen slices were stained using hematoxylin, eosin Y and safranin.

2.2.13. STATISTICAL ANALYSIS

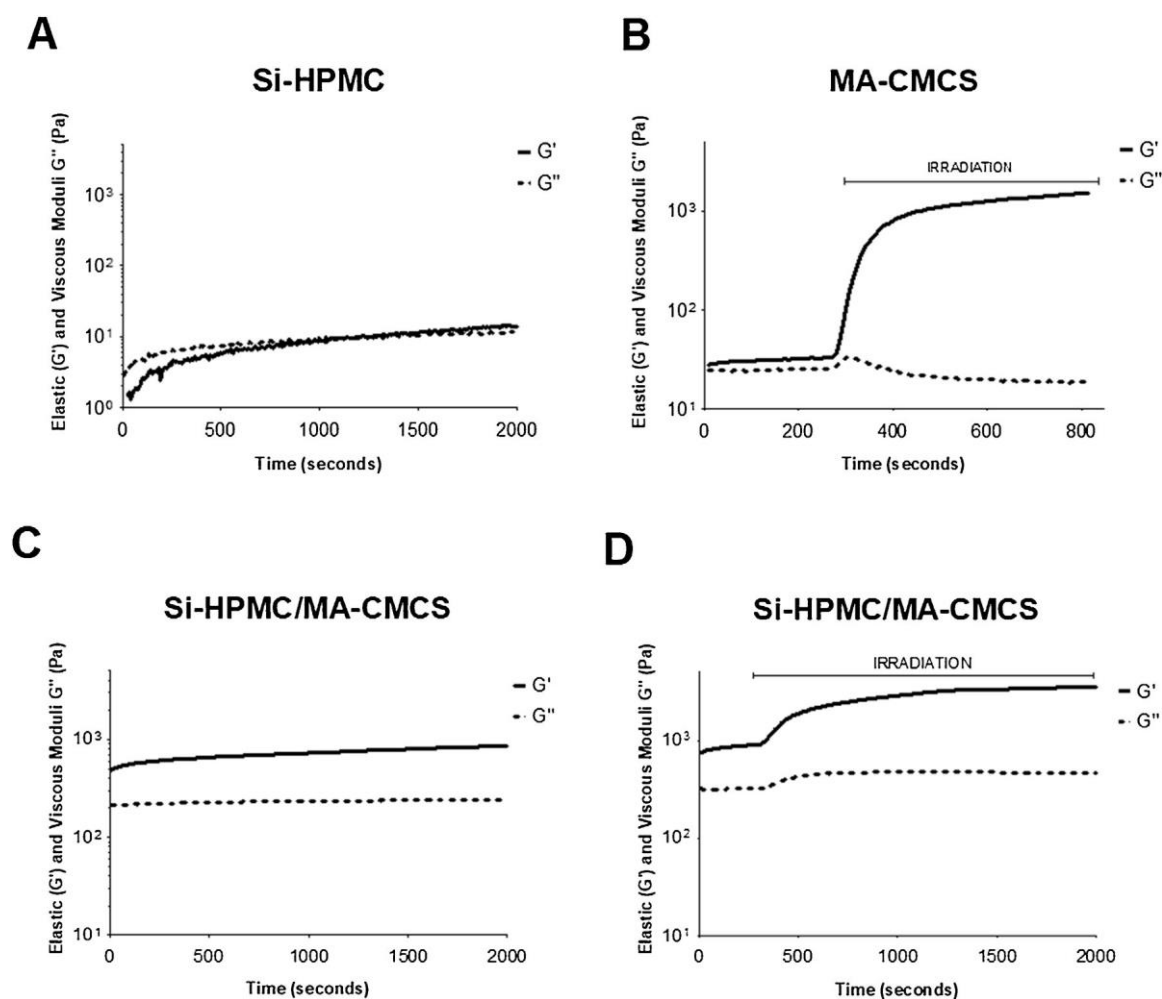
GraphPad 6 was used to perform statistical analysis on cytocompatibility tests using the two-way ANOVA Bonferroni test and on rheological-mechanical tests with a one-way ANOVA post Tukey test.

Figure 1.



Synthesis diagram of methacrylated carboxymethyl chitosan (MA-CMCS) and silanized hydroxypropyl methylcellulose (Si-HPMC).

Figure. 2



Variation of elastic and viscous moduli of polymer solutions as a function of time (seconds) of (A) Si-HPMC without irradiation, (B) MA-CMCS with irradiation, (C) Si-HPMC/MA-CMCS without irradiation and (D) Si-HPMC/MA-CMCS with irradiation. Data recorded at 6.8 rad/s frequency, 1% strain, room temperature; the lamp used for irradiation with $\lambda = 450$ nm, 430 mW, 350 mA. Si-HPMC: silanized hydroxypropyl methylcellulose, MA-CMCS: methacrylated carboxymethyl chitosan, Si-HPMC/MA-CMCS: silanized hydroxypropyl methylcellulose/methacrylated carboxymethyl chitosan.

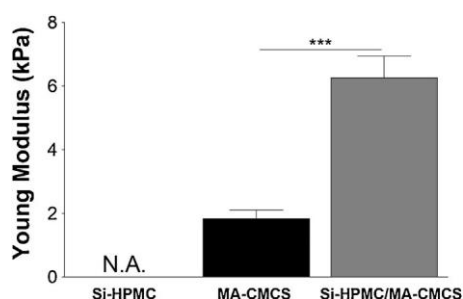
3. Results

3.1. CHEMICAL CHARACTERIZATION

In this study we developed an interpenetrating polymer network to make an *in situ* photocrosslinkable hydrogel membrane. Previous work demonstrated the good cell barrier effect of Si-HPMC; however, certain characteristics limit the use for this application. The addition of MA-CMCS combines its favorable properties with the Si-HPMC properties, such as photosensitivity and a degradable backbone.

The CMCS was modified as described in Fig. 1 to introduce photocrosslinkable moieties, i.e., methacrylic groups, providing phototriggered crosslinking ability to the material. FTIR and ^1H NMR confirmed the grafting of methacrylic pendant groups onto CMCS backbone. On the infrared spectrum, the peak of methacrylate carbonyl group appears at 1723cm^{-1} . After reaction with glycidyl methacrylate, three new signals also appear on the ^1H NMR spectra, compared to the spectrum of the starting CMCS, corresponding to the CH₃ at 2.5 ppm and 6.3 ppm, and the 6.75 ppm peaks of double-bond protons of the grafted methacrylate groups. The integration of peaks compared to the 2.6 ppm peak of the methyl group of the acetyl group in carboxymethyl chitosan confirms a grafting density around 35% (Fig. S1 in the online version, at DOI:10.1016/j.dental.2018.09.017).

Figure 3.



Mechanical characterization of photochemically cross-linked hydrogel (120 s with a visible light lamp). Young modulus obtained in compression experiment for Si-HPMC, MA-CMCS and Si-HPMC/MA-CMCS after photocrosslinking (mean value \pm SEM, $n=3$). Statistical analysis was performed with one-way ANOVA with post-Tukey test (** $p < 0.001$). Si-HPMC: silanized hydroxypropyl methylcellulose, MA-CMCS: methacrylated carboxymethyl chitosan, Si-HPMC/MA-CMCS: silanized hydroxypropylmethylcellulose/methacrylated carboxymethylchitosan.

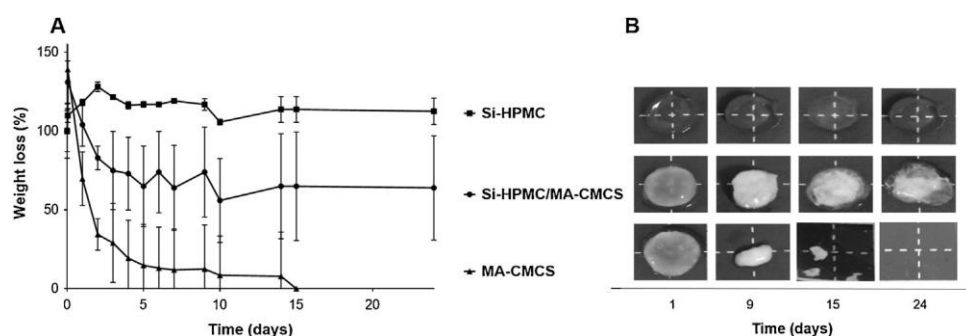
3.2. RHEOLOGICAL AND MECHANICAL PROPERTIES

Fig. 2 shows the elastic and viscous moduli as a function of time (seconds) of four different systems: Si-HPMC (1.14% (w/v) without irradiation), MA-CMCS (2.86% (w/v) with irradiation after 300 s), Si-HPMC/MA-CMCS (1.14%/2.86% (w/v) without irradiation) and Si-HPMC/MA-CMCS (1.14%/2.86% (w/v) with irradiation after 300 s). As expected, the Si-HPMC sample (Fig. 2A) shows a gradual increase of both moduli with time as a consequence of the crosslinking by silanol condensation. This increase of moduli is relatively slow with a crossover of the moduli only achieved after 15 min. In the MA-CMCS sample (Fig. 2B) the elastic modulus is already higher than the viscous modulus at the beginning of the measurement, with a small difference between them, suggesting the existence of physical interactions between the MA-CMCS chains. The moduli remain constant without irradiation (0–300 s) showing that no reaction occurs in these conditions. Interestingly, a sharp and immediate increase of the elastic modulus is observed with stabilization around 103 Pa after less than 100–200 s. These results confirm the potential of MA-CMCS to quickly cross-link upon irradiation. To impart this potential to the Si-HMPC membranes, MA-CMCS has been added to reach a Si-HMPC/MA-CMCS 1.14%/2.86% (w/v) ratio. This ratio was chosen after preliminary results that showed that the smaller amount of MA-CMCS does not efficiently crosslink the membrane upon irradiation. At the beginning of the measurement, the moduli were significantly higher than those observed with the individual

component demonstrating that interactions occur between both components. Without irradiation (Fig. 2C), a small increase of the moduli is observed due to the silanol condensation of Si-HPMC. When the irradiation starts (after 300 s in Fig. 2D), a sharp and immediate increase of the moduli is observed to reach a plateau around 103–104 Pa. The stability of the MA-CMCS and Si-HPMC/MA-CMCS hydrogels was confirmed by frequency sweep measurement after 120 s of irradiation (Fig. S2 in the online version, at DOI:10.1016/j.dental.2018.09.017). A plateaulike behavior is observed in both cases with no decrease of the storage modulus at low frequencies.

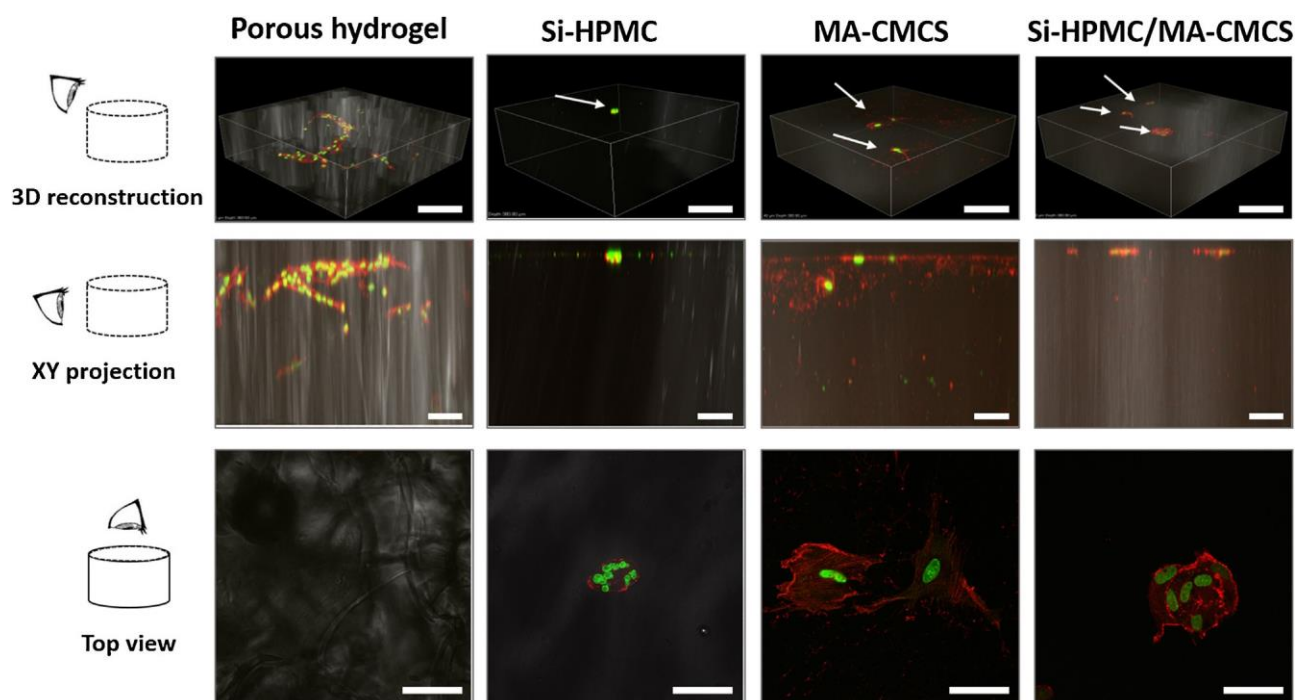
Mechanical compression tests were performed on the different samples after 120 s upon irradiation. As expected Si-HPMC was not sufficiently cross-linked after 120 s to perform this analysis, confirming that the second polymer network was necessary to obtain a liquid-to-solid material with a fast gelification time. The Si-HPMC/MA-CMCS (1.14%/2.86% (w/v)) samples show a significantly higher compression modulus than the MA-CMCS (2.86% (w/v)) material, suggesting that the double network improves the mechanical properties of the hydrogel (Fig. 3).

Figure 4.



Degradation profile of Si-HPMC, MA-CMCS and Si-HPMC/MA-CMCS hydrogels in presence of lysozyme. (A) Weight loss of hydrogels incubated in lysozyme solution (10 mg/mL in PBS), at 37°C, was assessed as a function of time. Results are expressed as a percentage of the initial weight (mean value \pm SEM, $n = 3$). (B) Representative pictures of hydrogels taken after 1, 9, 15 and 24 days of incubation. Si-HPMC: silanized hydroxypropyl methylcellulose, MA-CMCS: methacrylated carboxymethyl chitosan, Si-HPMC/MA-CMCS: silanized hydroxypropyl methylcellulose/methacrylated carboxymethyl chitosan.

Figure 5.



Hydrogel barrier effect against primary human gingival fibroblasts. Confocal microscopy images of porous hydrogel, Si-HPMC hydrogel, MA-CMCS hydrogel and Si-HPMC/MA-CMCS hydrogel after 4 days in culture with cells seeded on the top surface (nuclear staining: Yoyo-1; actin staining: phalloidin-Alexa Fluor 568). Top: 3D reconstruction of volume observed from hydrogel top surface to a 300 μ m thickness. Cells on the surface are indicated by arrows. Scale bar = 300 μ m. Middle: XY projection of the volume observed. Scale bar = 150 μ m. Bottom: hydrogel on the top surface of biomaterials. Scale bar = 50 μ m. Si-HPMC: silanized hydroxypropyl methylcellulose, MA-CMCS: methacrylated carboxymethyl chitosan, Si-HPMC/MA-CMCS: silanized hydroxypropyl methylcellulose/methacrylated carboxymethyl chitosan.

3.3. ENZYME DEGRADATION

Hydrogel membrane degradation was evaluated following the weight loss in presence of lysozyme solution (10 mg/mL) over a period of 24 days. Fig. 4A shows that cross-linked Si-HPMC

hydrogel maintained a stable weight throughout the observation time. MA-CMCS started to lose weight after 1 day of incubation in lysozyme. The weight reduced progressively until insoluble fragments were formed at day 15. When we combined the two polymers, forming IPN, the hydrogel membrane showed a reduction in weight compared to Si-HPMC hydrogel; however, the reduction proceeded more slowly than with the MA-CMCS hydrogel.

Comparing the pictures taken during degradation experiments (Fig. 4B), the Si-HPMC results were stable for all the observations in its shape and its transparent appearance. MA-CMCS, on the other hand, appeared whiter compared to Si-HPMC. The addition of MA-CMCS to Si-HPMC biomaterial increased, at first, the whiter aspect of hydrogel and successively a transparent part appeared in the border area. Observing the weight loss and the pictures, the degradation seemed to proceed with a surface erosion mechanism. The presence of a CMCS network in the hydrogel membrane, in the lysozyme solution, made it possible to obtain a progressive decrease in weight loss compared to Si-HPMC hydrogel.

3.4. IN VITRO CELL VIABILITY

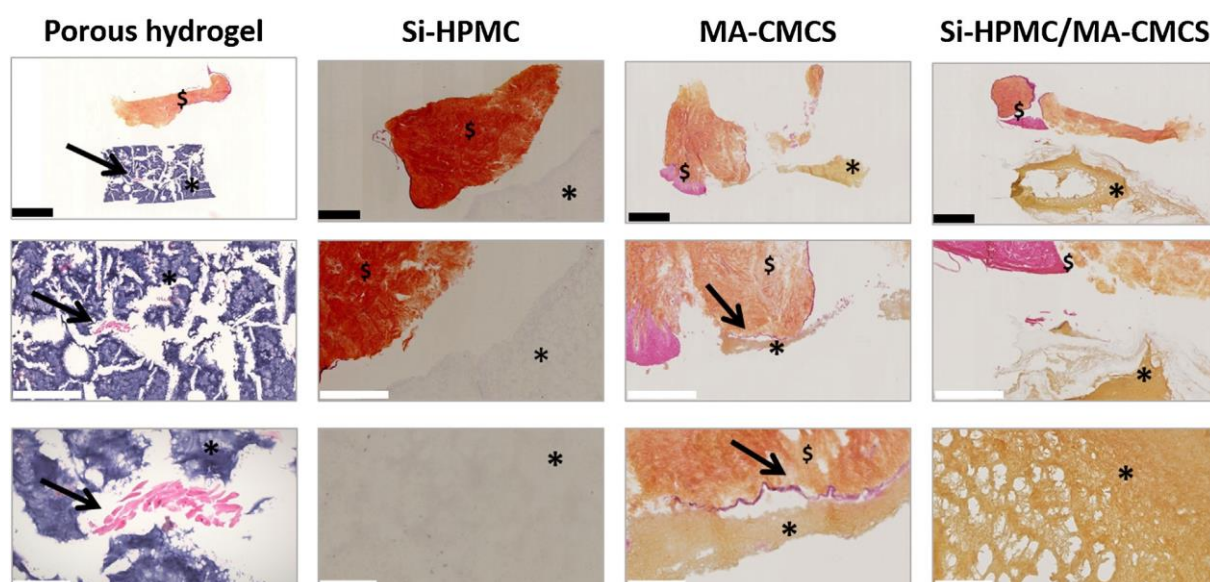
In this study we prepared a multicomponent hydrogel membrane for GTR. The cytocompatibility of the components and hydrogel were analyzed.

Firstly, we measured the influence on cell viability of the PIS under visible light curing irradiation for 120 s. Untreated cells were used as a positive control of cytocompatibility. The results (Fig. S3A in the online version, at DOI:10.1016/j.dental.2018.09.017) show that, after 24 h from contact with PIS, whether or not it was irradiated, the neutral red uptake of untreated cells was comparable with the cells in the experimental conditions.

MA-CMCS was synthesized to bring a particular synergistic combination of properties to Si-HPMC. After synthesis an extract of MA-CMCS polymer was made to assess the cytocompatibility. The extract was added to cell medium at 10% (v/v). Neutral red uptake of cells was evaluated after 24 and 72 h of contact between cells and polymer extract and 120 s of lamp exposure. All the results of the experimental conditions were compared to the untreated cells. No variation in neutral red uptake was evidenced for extract presence or for irradiation (Fig. S3B in the online version, at DOI:10.1016/j.dental.2018.09.017).

Lastly, cytocompatibility of cells in contact 24 and 72 h with Si-HPMC, MA-CMCS and Si-HPMC/MA-CMCS hydrogels was evaluated. Neutral red uptake results were compared to cell cultured without hydrogel. No significant differences were found between the viability of cells alone and the cultured cells in contact with Si-HPMC, MA-CMCS and Si-HPMC/MA-CMCS hydrogel membrane (Fig. S3C in the online version, at DOI:10.1016/j.dental.2018.09.017).

Figure 6.



Hydrogel barrier effect against human gingival tissue. Histological sections of gingiva explant were cultured with porous hydrogel, Si-HPMC hydrogel, MA-CMCS hydrogel and Si-HPMC/MA-CMCS hydrogel. The hydrogels were maintained in contact with the explants in culture for 1 week. (Histological staining: hematoxylin, eosin Y and safranin). Asterisk = hydrogel, dollar sign = explant, arrow = cell infiltrate/in contact with hydrogel. Scale bar: top = 1 mm, middle = 250 μm, bottom = 50 μm. Si-HPMC: silanized hydroxypropyl methylcellulose, MA-CMCS: methacrylated carboxymethyl chitosan, Si-HPMC/MA-CMCS: silanized hydroxypropyl methylcellulose/methacrylated carboxymethyl chitosan.

3.5. *IN VITRO* CELL BARRIER EFFECT

The cell barrier effect is one of the most important characteristics of the material to be used as a membrane for GTR. To prove the cell obstruction, human gingival fibroblasts were seeded on the top of hydrogels for 4 days. The hydrogels were analyzed as the above-mentioned conditions. In Fig. 5 (top), 3D reconstructions of the Z-stack of the top surface in contact with cells up to 300 μm thick are reported; in the middle a 2D projection from a lateral view of volume is reported; and on the bottom pictures of hydrogels' top surface are reported. A porous pullulan/dextran hydrogel was used as a negative control in which cells are able to infiltrate the biomaterial. Fig. 5 shows that cells were found in the volume and no cells are observable at the material's surface. On the Si-HPMC sample, the cells are found on top of the biomaterial, round in shape and organized in a cluster. From the lateral projection view, the barrier effect of Si-HPMC is clearly confirmed. On MA-CMCS, cells are also found on top but are more elongated, suggesting a different interaction between cells and the hydrogel. From a lateral projection, the barrier effect is confirmed compared to porous hydrogel. Si-HPMC/MA-CMCS presented cells on the hydrogel surface organized in groups with a rounded appearance, but more extended than Si-HPMC. From the lateral view, the occlusive aspect of the biomaterials is confirmed and it is similar to the occlusive aspect of Si-HPMC.

3.6. *EX VIVO* MODEL

Further investigation on the cell barrier effect analyzed *ex vivo* gingiva explant cultured in contact with hydrogels. In Fig. 6, histological sections after staining are reported. Gingival explants appear on a more yellow/orange layer due to the collagen composition, surmounted by a rich pink layer of cells. Porous pullulan/dextran hydrogel was used as a negative control of the material, in which cells are able to infiltrate the volume. Porous hydrogel presents cells inside the biomaterials shown by arrows. Si-HPMC hydrogel remains transparent after staining, however, a visual analysis was possible, confirming that no cells were inside the biomaterial. MA-CMCS appears yellow/orange, similar to the explant. The material was found partially in contact with the biological tissue (shown by arrow), suggesting the different interaction between tissue and hydrogel, as already observed with human gingival fibroblasts in contact with MA-CMCS hydrogel. The Si-HPMC/MA-CMCS hydrogel membrane also appears in yellow/brown and no cells were visible inside the biomaterial.

The Si-HPMC hydrogel was already proved *in vivo* in an animal model to possess a barrier effect against soft tissue cell invasion. In this experiment this property was confirmed and also MA-CMCS and IPN hydrogel showed cell occlusion against cell infiltration compared to hydrogel with macroporosity, which is not adapted for this kind of application.

4. Discussion

In this study, we developed a liquid mixture able to cross-link under irradiation with a standard dentist's lamp into an interpenetrated polymer network hydrogel membrane composed of Si-HPMC and MA-CMCS for GTR in periodontal defects. Si-HPMC is a functional polymer able to undergo, at

neutral pH, a condensation reaction that results in the formation of a three-dimensional network [30,37]. This viscoelastic polymer can be injected as a viscous solution and then build a 3D network *in situ*. Previous work in periodontal defects in an animal model demonstrated its ability to act as a physical barrier against cell invasion [38]; however, a fast crosslinking reaction is required for this application.

An interpenetrated polymer network was made because it presents a synergistic combination of the favorable properties of each of the polymer networks. Si-HPMC was selected to assess the barrier effect against gingival tissue invasion and CMCS allows the modification of membrane degradation due to its degradable backbone. In addition, the methacrylate grafted chains on CMCS can cure the biomaterial in a short period of time. MA-CMCS was synthesized to impart the photosensitivity to the formulation. FT-IR and NMR peaks confirm the functionalization reaction on CMCS backbone. No specific grafting site was targeted, but a random distribution was sought. In the literature the reaction between glycidyl methacrylate (GMA) and many polysaccharides has been reported. Van Dijk-Wolthuis studied the reaction between GMA and Dextran. He demonstrated by NMR studies that two reactions are in competition the ring opening of epoxide and a transesterification reaction between the hydroxyl groups of polymer and the carbonyl of methacrylic groups [39]. Furthermore, Elisseeff, reported about the reaction of GMA and chondroitin-sulphate, that the transesterification reaction is a rapid reversible reaction, in contrast to the ring-opening product which slowly appears along the time [40,41]. In addition, Hutmacher described that in presence of free amino groups, such as gelatin polymer, GMA preferentially reacts with them in a percentage about 90% of all the grafted functionality [42]. In 2007, Poon successfully grafted methacrylate groups onto CMCS by reaction of CMCS with glycidyl methacrylate in water under basic conditions. The ¹H and ¹³C NMR spectra of the collected MA-CMCS confirmed the grafting of methacrylate groups by transesterification or transamidation mechanisms and not by the ring-opening of the epoxide of glycidyl methacrylate. The ¹H NMR spectrum (Fig. S1 in the online version, at DOI:10.1016/j.dental.2018.09.017) recorded on our sample confirms the successful grafting of methacrylic bonds but does not allow to determine undoubtedly by which reaction (transamidation/transesterification) it occurs. Moreover, we cannot exclude that a part of the grafted methacrylic groups is coming from the ring-opening of the epoxide by the amino groups. However, independently from mechanisms, the content of methacrylate groups randomly grafted on CMCS backbone required for the targeted mechanical and gelification properties was reached.

To photocrosslink our biomaterials, we chose to use a dentistry visible light lamp (420–480 nm). This lamp is already used by dentists to cure composites for dental restoration.

Photocrosslinking uses light to dissociate the photoinitiator into radicals, which can propagate to macromolecules. The ratio between the polymers and the photoinitiator concentration is a key point for successful crosslinking. In addition, the concentration of the photoinitiator is not excessive, thus preventing phototoxicity consequences. At the beginning of the project, camphorquinone was tested to initiate the radical reaction; however, overly long irradiation was required with this photoinitiator. We then attempted the riboflavin molecule but rapidly switched to its phosphate derivatives. Riboflavin 5-phosphate sodium salt hydrate, given its higher water solubility, avoids the

use of organic solvent or ethanol, often used to solubilize the photoinitiator as reported in the literature [43]. When the use of RP as photoactivator was considered, triethanolamine was used as a coinitiator. This molecule is described in the literature by Previtali et al. as being more efficient as the alkyl-substituted amine [44].

The *in situ* formation of hydrogel membrane remarkably differs from what is available today on the market. To our knowledge, all the membranes used for GTR are in solid form and they need to be adapted by the dentist in their shape before implantation. The liquid formulation, able to form a solid membrane *in situ*, is an easy-to-use material, especially for complicated shapes or for a defect that is difficult to reach. In addition, a better shape adaption to the wound could increase the intimate contact with the defect and consequently improve the cell barrier effect compared to solid membranes. Rheological analysis of Si-HPMC/MA-CMCS showed a strong decrease in gelling time compared to Si-HPMC alone with the advantage of being able to control the start of the crosslinking with the start of irradiation. The combination between the two polymers and the PIS results in an IPN hydrogel membrane after 2 min of irradiation, compared to Si-HPMC in which the gel point appears after 15 min. Gelation seems coherent with the gel time already found in the literature with riboflavin and a visible light lamp [26,28,29,45,46].

IPN materials, which can be obtained by either chemical or physical crosslinking, in most cases show physicochemical properties that can differ remarkably from those of the macromolecular constituents [47,48]. MA-CMCS and SiHPMC/MA-CMCS were analyzed under uniaxial compression after 120 s of irradiation. As expected at this time, Si-HPMC alone was not sufficiently cross-linked to perform this analysis, confirming a second polymer network is required to obtain a liquid-to-solid material that is adapted to clinical conditions in a few minutes. The compression test showed similar values to the study reported in the literature and the mechanical increase in stiffness seems coherent with the presence of second polymer network formation [26,49,50]. The formation of the IPN enhances the mechanical strength of the composite hydrogel.

An ideal membrane is described as a biocompatible material, to avoid tissue response, preferably biodegradable to avoid a second surgical intervention, acting as a soft tissue physical barrier, but also clinically manageable. Phototoxicity (photoirritation) is an acute light-induced tissue response to a photoreactive chemical. Excitation of molecules by light can lead to generating reactive species (ROS). We therefore assessed the photo safety of the new material by neutral red uptake [43,51–53]. We analyzed the cytocompatibility using murine fibroblasts and we measured the neutral red uptake on cells after incubation with the PIS, the MA-CMCS extract and hydrogels. A photoinitiator, under irradiation, gives radical species to react with the methacrylate unsaturated groups. The results showed that the PIS at this concentration, in combination with the time of irradiation chosen, did not demonstrate diminution of cytocompatibility compared with the untreated cells. Also, the contact between the cells and the polymer extract or in contact with Si-HPMC, MA-CMCS and Si-HPMC/MA-CMCS hydrogel membrane did not exhibit a decrease in cell viability compared to values found for cells cultured without biomaterials.

The degradation rate is a key point in membrane for GTR. Chitosan can be degraded with human enzymes such as lysozyme. The degradation could be impacted with factors that modify its water

solubility, such as the degree of deacetylation or cross-linked chains [54]. To determine the influence of two-polymer materials, cross-linked hydrogels were placed in high concentrated lysozyme solution in physiological conditions. Lysozyme is the common enzyme used to study chitosan degradation [55,56], it is produced by cells and it is contained in saliva in different amounts depending on patients' habits and conditions. Glycol methacrylate chitosan was treated with lysozyme by Shapka [57]. The concentration was 4 mg/mL and the hydrogels with different degrees of substitution were incubated for 5 months, without complete degradation. Lee and co-workers analyzed the effect of glycol methacrylate chitosan mixed with hyaluronic acid. However, their hydrogels made of glycol methacrylate chitosan did not completely degrade in the 42-day observation time, and in the composite hydrogel they observed a slower gel mass loss. The comparison between experimental studies appears difficult due to the different chitosan types, degrees of modification, photoinitiators and irradiation conditions. They appear to have in common the difficulty in the enzyme diffusion in the volume in relationship with a more cross-linked network or a denser network for the addition of second polymer [26]. In the current study, we followed the weight variation of crosslinked Si-HPMC, MA-CMCS and Si-HMCP/MA-CMCS hydrogel membrane in lysozyme solutions. Si-HPMC was selected to assess the barrier effect against gingival tissue invasion, and CMCS allows the modification of membrane degradation due to its degradable backbone. We confirmed that the presence of the CMCS network in membrane can reach a progressive mass loss, compared with Si-HPMC, which is stable throughout the experiment. The critical time for soft tissue cell migration has been reported to be 14 days, the length of time the membrane has to be intact for wound healing. MA-CMCS hydrogel alone reduces its mass until the formation of fragments at day 15, making it poorly adapted to be used alone for this membrane application. In the current experiment, the stability of Si-HPMC and the degradability of MA-CMCS could be balanced in a favorable combination of the two polymer networks.

In GTR, the membrane has to have a resorption time compatible with tissue regeneration, but has to act as a physical barrier against soft tissue cells. To assess the barrier effect of IPN hydrogel membrane, we conducted two experiments. For the first experiment, isolated human gingival fibroblasts were seeded on top of hydrogel. After culture, cells were observed by confocal microscopy. In Si-HPMC and Si-HPMC/MA-CMCS cross-linked material, cells were found on the top surface of the biomaterial, within the cluster, but they were not able to enter the volume, confirming the barrier effect. In MA-CMCS cells appear more elongated and in the area of observation, from observation of lateral projection, a cell seems to start infiltrating the hydrogel volume. This could be related to a different interaction between cells and MA-CMCS hydrogel or to a degradation rate of chitosan backbone. In the second experiment, human gingiva explant was cultured in contact with biomaterials for 1 week and then analyzed using histological staining. The results confirmed that the cells could not infiltrate the cross-linked hydrogels. Porous hydrogels were used as a negative control in both experiments. Isolated cells and cells from soft tissue have been able to infiltrate the biomaterial. Cells were found in groups inside the volume, probably passing through the hydrogel macroporosity. The comparison between IPN and control hydrogel showed the strong correlation between the hydrogel structure and the cell's occlusive potential, demonstrating that IPN hydrogel could be an adapted membrane for GTR. In previous experiments, we used Si-HPMC as a self-setting

hydrogel for cell encapsulation. The *in vitro* results confirm the ability of SiHPMC to act as a physical barrier trapping cells inside the hydrogel. In addition, cell viability was demonstrated up to 21 days and diffusion experiments confirm the possibility of nutrient diffusion, essential for cell survival [14,58–60]. These previous experiments could be correlated with the *in vitro/ex vivo* results found in this study. In fact, due to the presence of Si-HPMC, the cells cannot cross the hydrogel barrier, maintaining cell viability. These physical barrier properties are also confirmed in several *in vivo* studies [60]. Moreover, the results obtained in periodontal lesions in dogs treated with crosslinked Si-HPMC membrane suggested that the hydrogel may act as an occlusive barrier to protect bone area from soft connective tissue invasion. However, the placement and adaptation of this membrane is described as being quite difficult during the surgical phase [61]. Hence, *in situ* curing hydrogel membrane may be the most appropriate strategy to overcome these limitations.

The two experiments conducted on the barrier effect of IPN could be a preliminary alternative to study the biomaterial barrier effect *in vitro*. However, we intend to conduct detailed animal studies to confirm the characteristics discussed in this paper and explore the potential of *in situ* IPN hydrogel membrane in an *in vivo* animal model of periodontitis.

5. Conclusion

The aim of this study was to develop an innovative *in situ* hydrogel membrane for GTR of periodontal defects. A previous study demonstrated the capability of Si-HPMC to act as a physical barrier against cell invasion in periodontal defects. However, the crosslinking rate was not well adapted for this clinical application. Therefore, we developed an innovative mixture by adding a biodegradable polymer to Si-HPMC that can be cross-linked photochemically, namely MA-CMCS. We used a photoinitiator based on riboflavin phosphate and visible light lamp (420–480 nm), already used in dentistry. With the presence of this second polymer in the injectable viscous solution, the system becomes phototriggered, reducing the gelation time drastically in agreement with clinical needs. The resulting IPN hydrogel presents reinforced mechanical properties with preserved biocompatibility. This mixture is easy to handle because it is possible to apply it and cross-link it *in situ* using a common dentistry lamp. In addition, the presence of a chitosan polymer increases the degradability of the resulting biomaterial, making it possible to find a favorable combination of different polymer networks and to tune the degradation time in the future in accordance with *in vivo* needs. The results of the *in vitro* test and histological analysis confirm the biocompatibility of the material and the barrier effect against soft tissue cell invasion.

Acknowledgements

We would like to acknowledge Dr. Alexandra Cloitre for isolated human gingival fibroblasts.

We would like to acknowledge the MicroPCell Facility (SFR santé Franc, ois Bonamy -IRS UN).

This work is supported by Erasmus Mundus Doctoral School Nanofar from the European Community and POsTURE project from EuroNanoMed II.

References

- [1] Albandar JM, Rams TE. Global epidemiology of periodontal diseases: an overview. *Periodontol* 2000 2002;29:7–10, <http://dx.doi.org/10.1034/j.1600-0757.2002.290101.x>.
- [2] de Oliveira C, Watt R, Hamer M. Toothbrushing, inflammation, and risk of cardiovascular disease: results from Scottish health survey. *BMJ* 2010;340:c2451, <http://dx.doi.org/10.1136/bmj.c2451>.
- [3] Cullinan MP, Seymour GJ. Periodontal disease and systemic illness: will the evidence ever be enough? *Periodontol* 2000 2013;62:271–86, <http://dx.doi.org/10.1111/prd.12007>.
- [4] Hugoson A, Norderyd O. Has the prevalence of periodontitis changed during the last 30 years? *J Clin Periodontol* 2008;35:338–45, <http://dx.doi.org/10.1111/j.1600-051X.2008.01279.x>.
- [5] Socransky SS, Haffajee AD. The bacterial etiology of destructive periodontal disease: current concepts. *J Periodontol* 1992;63:322–31, <http://dx.doi.org/10.1902/jop.1992.63.4s.322>.
- [6] Gross AJ, Paskett KT, Cheever VJ, Lipsky MS. Periodontitis: a global disease and the primary care provider's role. *Postgrad Med J* 2017:1–6, <http://dx.doi.org/10.1136/postgradmedj-2017-134801>.
- [7] Bottino MC, Thomas V, Schmidt G, Vohra YK, Chu TG, Kowolik MJ, et al. Recent advances in the development of GTR/GBR membranes for periodontal regeneration — a materials perspective. *Dent Mater* 2012;28:703–21, <http://dx.doi.org/10.1016/j.dental.2012.04.022>.
- [8] Sheikh Z, Qureshi J, Alshahrani AM, Nassar H, Ikeda Y, Glogauer M, et al. Collagen based barrier membranes for periodontal guided bone regeneration applications. *Odontology* 2017;105:1–12, <http://dx.doi.org/10.1007/s10266-016-0267-0>.
- [9] Wang J, Wang L, Zhou Z, Lai H, Xu P, Liao L, et al. Biodegradable polymer membranes applied in guided bone/tissue regeneration: a review. *Polymers (Basel)* 2016;8:1–20, <http://dx.doi.org/10.3390/polym8040115>.
- [10] Dimitriou R, Mataliotakis GI, Calori GM, Giannoudis PV. The role of barrier membranes for guided bone regeneration and restoration of large bone defects: current experimental and clinical evidence. *BMC Med* 2012;10:81, <http://dx.doi.org/10.1186/1741-7015-10-81>.
- [11] Jung RE, Hälg GA, Thoma DS, Hämmerle CHF. A randomized, controlled clinical trial to evaluate a new membrane for guided bone regeneration around dental implants. *Clin Oral Implants Res* 2009;20:162–8, <http://dx.doi.org/10.1111/j.1600-0501.2008.01634.x>.
- [12] Coonts BA, Whitman SL, Donnell MO, Polson AM, Bogle G, Garrett S, et al. Biodegradation and biocompatibility of a guided tissue regeneration barrier membrane formed from a liquid polymer material. *J Biomed Mater Res* 1998;42(November (2)):303–11.
- [13] Fella BH, Fatimi A, Quillard S, Vinatier C, Gauthier O, Janvier P, et al. Biomaterials The *in vivo* degradation of a ruthenium labelled polysaccharide-based hydrogel for bone tissue engineering. *Biomaterials* 2009;30:1568–77, <http://dx.doi.org/10.1016/j.biomaterials.2008.11.031>.
- [14] Mathieu E, Lamirault G, Toquet C, Lhomme P, Rederstorff E, Sourice S, et al. Intramyocardial delivery of mesenchymal stem cell-seeded hydrogel preserves cardiac function and attenuates ventricular remodeling after myocardial infarction. *PLoS One* 2012;7, <http://dx.doi.org/10.1371/journal.pone.0051991>.
- [15] Trojani C, Weiss P, Michiels JF, Vinatier C, Guicheux J, Daculsi G, et al. Three-dimensional culture and differentiation of human osteogenic cells in an injectable hydroxypropylmethylcellulose hydrogel. *Biomaterials* 2005;26:5509–17, <http://dx.doi.org/10.1016/j.biomaterials.2005.02.001>.

- [16] Merceron C, Portron S, Masson M, Lesoeur J, Fella BH, Gauthier O, et al. The effect of two and three dimensional cell culture on the chondrogenic potential of human adipose-derived mesenchymal stem cells after subcutaneous transplantation with an injectable hydrogel. *Cell Transplant* 2011;20:1575–88, <http://dx.doi.org/10.3727/096368910X557191>.
- [17] Struillou X, Boutigny H. Treatment of periodontal defects in dogs using an injectable composite hydrogel/biphasic calcium phosphate. *J Mater Sci Mater Med* 2011;1707–17, <http://dx.doi.org/10.1007/s10856-011-4344-1>.
- [18] Anseth KS, Burdick JA. New directions in photopolymerizable biomaterials. *Mrs Bull* 2002;27:130–6, <http://dx.doi.org/10.1557/mrs2002.49>.
- [19] Nguyen KT, West JL. Photopolymerizable hydrogels for tissue engineering applications. *Biomaterials* 2002;23:4307–14, [http://dx.doi.org/10.1016/S0142-9612\(02\)00175-8](http://dx.doi.org/10.1016/S0142-9612(02)00175-8).
- [20] Matricardi P, Di Meo C, Coviello T, Hennink WE, Alhaique F. Interpenetrating polymer networks polysaccharide hydrogels for drug delivery and tissue engineering. *Adv Drug Deliv Rev* 2013;65:1172–87, <http://dx.doi.org/10.1016/j.addr.2013.04.002>.
- [21] Valmikinathan CM, Mukhatyar VJ, Jain A, Karumbaiah L, Dasari M, Bellamkonda RV. Photocrosslinkable chitosan based hydrogels for neural tissue engineering. *Soft Matter* 2012;8:1964–76, <http://dx.doi.org/10.1039/C1SM06629C>.
- [22] Amoozgar Z, Rickett T, Park J, Tucheck C, Shi R, Yeo Y. Semi-interpenetrating network of polyethylene glycol and photocrosslinkable chitosan as an in-situ-forming nerve adhesive. *Acta Biomater* 2012;8:1849–58, <http://dx.doi.org/10.1016/j.actbio.2012.01.022>.
- [23] Viguiet A, Boyer C, Chassenieux C, Benyahia L, Guicheux J, Weiss P, et al. Interpenetrated Si-HPMC/alginate hydrogels as a potential scaffold for human tissue regeneration. *J Mater Sci Mater Med* 2016;27:99, <http://dx.doi.org/10.1007/s10856-016-5709-2>.
- [24] Mourya VK, Inamdar NN, Tiwari A. Carboxymethyl chitosan and its applications. *Adv Mater Lett* 2010;1:11–33, <http://dx.doi.org/10.5185/amlett.2010.3108>.
- [25] Owens GJ, Singh RK, Foroutan F, Alqaysi M, Han C, Mahapatra C, et al. Progress in polymer science polymeric materials for bone and cartilage repair. *Carbohydr Polym* 2014;14:167–82, <http://dx.doi.org/10.1016/j.pmatsci.2015.12.001>.
- [26] Hu J, Hou Y, Park H, Choi B, Hou S, Chung A, et al. Visible light crosslinkable chitosan hydrogels for tissue engineering. *Acta Biomater* 2012;8:1730–8, <http://dx.doi.org/10.1016/j.actbio.2012.01.029>.
- [27] Nguyen AK, Gittard SD, Koroleva A, Schlie S, Gaidukeviciute A, Chichkov BN, et al. Two-photon polymerization of polyethylene glycol diacrylate scaffolds with riboflavin and triethanolamine used as a water-soluble photoinitiator. *Regen Med* 2013;8:725–38, <http://dx.doi.org/10.2217/rme.13.60>.
- [28] Kim SH, Chu CC. Visible light induced dextran-methacrylate hydrogel formation using (–)-riboflavin vitamin B2 as a photoinitiator and L-arginine as a co-initiator. *Fibers Polym* 2009;10:14–20, <http://dx.doi.org/10.1007/s12221-009-0014-z>.
- [29] Beztsinna N, Sole M, Taib N, Bestel I. Bioengineered riboflavin in nanotechnology. *Biomaterials* 2016;80:121–33, <http://dx.doi.org/10.1016/j.biomaterials.2015.11.050>.
- [30] Bourges X, Weiss P, Daculsi G, Legeay G. Synthesis and general properties of silylated-hydroxypropyl methylcellulose in prospect of biomedical use. *Adv Colloid Interface Sci* 2002;99:215–28, [http://dx.doi.org/10.1016/S0001-8686\(02\)00035-0](http://dx.doi.org/10.1016/S0001-8686(02)00035-0).
- [31] Fatimi A, Franc, ois Tassin J, Quillard S, Axelos MAV, Weiss P. The rheological properties of silylated hydroxypropylmethylcellulose tissue engineering matrices. *Biomaterials* 2008;29:533–43, <http://dx.doi.org/10.1016/j.biomaterials.2007.10.032>.

- [32] Fatimi A, Tassin JF, Axelos MAV, Weiss P. The stability mechanisms of an injectable calcium phosphate ceramic suspension. *J Mater Sci Mater Med* 2010;21:1799–809, <http://dx.doi.org/10.1007/s10856-010-4047-z>.
- [33] Engineering B, Zurich T, Engineering C, Engineering C, Company N, Introduction H. *In vitro* and *in vivo* performance of porcine islets encapsulated in interfacially photopolymerized poly (ethylene glycol) diacrylate membranes. *Cell Transplant* 1999;8:293–306.
- [34] Zuliani T, Saiagh S, Knol AC, Esbelin J, Dréno B. Fetal fibroblasts and keratinocytes with immunosuppressive properties for allogeneic cell-based wound therapy. *PLoS One* 2013;8, <http://dx.doi.org/10.1371/journal.pone.0070408>.
- [35] Grenade C, Moniotte N, Rompen E, Vanheusden A, Mainjot A, De Pauw-Gillet MC. A new method using insert-based systems (IBS) to improve cell behavior study on flexible and rigid biomaterials. *Cytotechnology* 2016;68:2437–48, <http://dx.doi.org/10.1007/s10616-016-9964-3>.
- [36] Lavergne M, Derkaoui M. Porous Polysaccharide-Based Scaffolds for Human Endothelial Progenitor Cells. *Macromol Biosci* 2012;901–10, <http://dx.doi.org/10.1002/mabi.201100431>.
- [37] Fatimi A, Tassin JF, Turczyn R, Axelos MAV, Weiss P. Gelation studies of a cellulose-based biohydrogel: the influence of pH, temperature and sterilization. *Acta Biomater* 2009;5:3423–32, <http://dx.doi.org/10.1016/j.actbio.2009.05.030>.
- [38] Struillou X, Boutigny H, Badran Z, Fellah BH, Gauthier O, Sourice S, et al. Treatment of periodontal defects in dogs using an injectable composite hydrogel/biphasic calcium phosphate. *J Mater Sci Mater Med* 2011;22:1707–17, <http://dx.doi.org/10.1007/s10856-011-4344-1>.
- [39] van Dijk-Wolthuis WNE, Kettenes-van den Bosch JJ, van der Kerk-van Hoof A, Hennink WE. Reaction of dextran with glycidyl methacrylate: an unexpected transesterification. *Macromolecules* 1997;30:3411–3, <http://dx.doi.org/10.1021/ma961764v>.
- [40] Wang D-A, Varghese S, Sharma B, Strehin I, Fermanian S, Gorham J, et al. Multifunctional chondroitin sulphate for cartilage tissue–biomaterial integration. *Nat Mater* 2007;6:385–92, <http://dx.doi.org/10.1038/nmat1890>.
- [41] Prado SS, Weaver JM, Love BJ. Gelation of photopolymerized hyaluronic acid grafted with glycidyl methacrylate. *Mater Sci Eng C* 2011;31:1767–71, <http://dx.doi.org/10.1016/j.msec.2011.08.008>.
- [42] Loessner D, Meinert C, Kaemmerer E, Martine LC, Yue K, Levett PA, et al. Functionalization, preparation and use of cell-laden gelatin methacryloyl based hydrogels as modular tissue culture platforms. *Nat Protoc* 2016;11:727–46, <http://dx.doi.org/10.1038/nprot.2016.037>.
- [43] Bryant SJ, Nuttelman CR, Anseth KS. Cytocompatibility of UV and visible light photoinitiating systems on cultured NIH/3T3 fibroblasts *in vitro*. *J Biomater Sci Polym Ed* 2012;11:439–57, <http://dx.doi.org/10.1163/156856200743805>.
- [44] Bertolotti SG, Previtali CM, Rufs AM, Encinas MV. Riboflavin/triethanolamine as photoinitiator system of vinyl polymerization. A mechanistic study by laser flash photolysis. *Macromolecules* 1999;32:2920–4, <http://dx.doi.org/10.1021/ma981246f>.
- [45] Kim S-H, Chu C-C. Fabrication of a biodegradable polysaccharide hydrogel with riboflavin, vitamin B2, as a photo-initiator and L-arginine as coinitorator upon UV irradiation. *J Biomed Mater Res B Appl Biomater* 2009;91:390–400, <http://dx.doi.org/10.1002/jbm.b.31414>.
- [46] Ahmad I, Iqbal K, Sheraz MA, Ahmed S, Mirza T, Kazi SH, et al. Photoinitiated polymerization of 2-hydroxyethyl methacrylate by riboflavin/triethanolamine in aqueous solution: a kinetic study. *ISRN Pharm* 2013 2013:958712, <http://dx.doi.org/10.1155/2013/958712>.

- [47] Matricardi P, Di Meo C, Coviello T, Hennink WE, Alhaique F. Interpenetrating polymer networks polysaccharide hydrogels for drug delivery and tissue engineering. *Adv Drug Deliv Rev* 2013;65:1172–87, <http://dx.doi.org/10.1016/j.addr.2013.04.002>.
- [48] Chen Q, Chen H, Zhu L, Zheng J. Materials chemistry B. Fundamentals of double network hydrogels. *J Mater Chem B* 2015;3:3645–886, <http://dx.doi.org/10.1039/C5TB00123D>.
- [49] Park H, Choi B, Hu J, Lee M. Injectable chitosan hyaluronic acid hydrogels for cartilage tissue engineering. *Acta Biomater* 2013;9:4779–86, <http://dx.doi.org/10.1016/j.actbio.2012.08.033>.
- [50] Arakawa C, Ng R, Tan S, Kim S, Wu B, Lee M. Photopolymerizable chitosan–collagen hydrogels for bone tissue engineering. *J Tissue Eng Regen Med* 2017;11:164–74, <http://dx.doi.org/10.1002/term.1896>.
- [51] Franz A, König F, Skolka A, Sperr W, Bauer P, Lucas T, et al. Cytotoxicity of resin composites as a function of interface area. *Dent Mater* 2007;23:1438–46, <http://dx.doi.org/10.1016/j.dental.2007.05.014>.
- [52] Consideration I. OECD Test Guideline 432: *In Vitro* 3T3 NRU Phototoxicity Test 2004:1–15. doi: <https://doi.org/10.1787/9789264071162-en>.
- [53] Bauer D, Averett LA, De Smedt A, Kleinman MH, Muster W, Pettersen BA, et al. Standardized UV–vis spectra as the foundation for a threshold-based, integrated photosafety evaluation. *Regul Toxicol Pharmacol* 2014;68:70–5, <http://dx.doi.org/10.1016/j.yrtph.2013.11.007>.
- [54] Croisier F, Jérôme C. Chitosan-based biomaterials for tissue engineering. *Eur Polym J* 2013;49:780–92, <http://dx.doi.org/10.1016/j.eurpolymj.2012.12.009>.
- [55] Ahmadi F, Oveisi Z, Samani SM, Amoozgar Z. Chitosan based hydrogels: characteristics and pharmaceutical applications. *Res Pharm Sci* 2015;10:1–16.
- [56] Guangyuan Lu, Baiyang Sheng, Gan Wang, Yujun Wei, Yandao Gong, Xiufang Zhang, et al. Controlling the degradation of covalently cross-linked carboxymethyl chitosan utilizing bimodal molecular weight distribution. *J Biomater Appl* 2008;23:435–51, <http://dx.doi.org/10.1177/0885328208091661>.
- [57] Amsden BG, Sukarto A, Knight DK, Shapka SN. Methacrylated glycol chitosan as a photopolymerizable biomaterial. *Biomacromolecules* 2007;8:3758–66, <http://dx.doi.org/10.1021/bm700691e>.
- [58] Hached F, Vinatier C, Pinta PG, Hulin P, Le Visage C, Weiss P, et al. Polysaccharide hydrogels support the long-Term viability of encapsulated human mesenchymal stem cells and their ability to secrete immunomodulatory factors. *Stem Cells Int* 2017;2017:6–8, <http://dx.doi.org/10.1155/2017/9303598>.
- [59] Nativel F, Renard D, Hached F, Pinta P, Arros CD, Weiss P, et al. Application of millifluidics to encapsulate and support viable human mesenchymal stem cells in a polysaccharide hydrogel. *Int J Mol Sci* 2018;19(7), <http://dx.doi.org/10.3390/ijms19071952>.
- [60] Moussa L, Pattappa G, Doix B, Benselama S, Demarquay C, Benderitter M, et al. A biomaterial-assisted mesenchymal stromal cell therapy alleviates colonic radiation-induced damage. *Biomaterials* 2017;115, <http://dx.doi.org/10.1016/j.biomaterials.2016.11.017>.
- [61] Struillou X, Fruchet A, Rakic M, Badran Z, Rethore G, Sourice S, et al. Evaluation of a hydrogel membrane on bone regeneration in furcation periodontal defects in dogs. *Dent Mater J* 2018, <http://dx.doi.org/10.4012/dmj.2017-238>.